IEEE Access
Multidisciplinary | Rapid Review | Open Access Journal

Received February 1, 2019, accepted February 22, 2019, date of publication February 26, 2019, date of current version March 13, 2019.

Digital Object Identifier 10.1109/ACCESS.2019.2901765

A Low-Profile and Wideband Unidirectional Antenna Using Bandwidth Enhanced Resonance-Based Reflector for Fifth Generation (5G) Systems Applications

BAO-JIAN WEN[1], LIN PENG[1,2], (Member, IEEE), XIAO-FENG LI[1], KUN-SHAN MO[3], XING JIANG[1], AND SI-MIN LI[4]

[1]Guangxi Key Laboratory of Wireless Wideband Communication and Signal Processing, Guilin University of Electronic Technology, Guilin 541004, China
[2]School of Physics, University of Electronic Science and Technology of China, Chengdu 610054, China
[3]School of Electronic Information and Automation, Guilin University of Aerospace Technology, Guilin 541004, China
[4]School of computer science and communication engineering, Guangxi University of Science and Technology, Liuzhou 545006, China

Corresponding author: Lin Peng (penglin528@hotmail.com)

This work was supported by the National Natural Science Foundation of China under Grant 61661011 and Grant 61761012.

ABSTRACT The previously proposed resonance-based reflector (RBR) antennas have the merits of wide impedance bandwidth, low-profile, and unidirectional pattern; however, their front-to-back ratio (FBR) bandwidths are narrow. In this paper, a wideband RBR is proposed for FBR bandwidth enhancing antenna with a low profile. The proposed RBR consists of a metallic ring with three stubs printed on a substrate. It has a $\pm 90^\circ$ in-phase bandwidth of 63.57% (3.23–6.24 GHz) and its reflection magnitude values range from -0.02 to -11.5 dB within the in-phase band ($-90^\circ < \varphi < 90^\circ$). Compared with the existent RBRs, the proposed RBR achieves a greater reflection magnitude within the in-phase band, which would be critical for FBR enhancement of an antenna. The proposed RBR is applied to a ring-loaded teardrop-shaped bowtie antenna to form unidirectional radiation pattern. The measured -10-dB impedance bandwidth of the proposed antenna is 3.48–6.12 GHz (55.00%), while FBR values are larger than 10 dB within the whole impedance band and the maximum FBR value is up to 20.4 dB. The peak gain is bigger than 7.3 dBi within the whole impedance band. There is a reasonable agreement between the simulated and measured results. The profile of the overall unidirectional antenna is $0.15\lambda_L$ at the lowest operating frequency, and the RBR has the same size as the bowtie antenna. Compared to the previous RBR antennas, the proposed RBR antenna has wider FBR bandwidth. The operating band of the antenna is suitable for 5G system applications.

INDEX TERMS Resonance-based reflector, low-profile antenna, wide band, unidirectional.

I. INTRODUCTION

Ultra-wide band (UWB) directional antennas are characterized by high security, good efficiency, low transmission power and high data rates, thus, more attentions have been paid to UWB directional antennas, which are also desired with the characteristics of compactness and low-profile. Such an antenna has a significant role in many applications, such as point to point communication, military services, wireless body area networks (WBAN) and microwave imaging [1]–[5]. Moreover, the 5G systems are expected to be deployed in the market beyond 2020 [6]. The frequency range of 3300–4200 MHz will be the primary band in the spectrum below 6 GHz for the global introduction of fifth generation (5G) reported by the Global mobile Supplier Association [7]. The potential frequency bands for 5G systems have been identified by Ofcom for range of 6 GHz and above [6]. Thus, to develop antennas that meet 5G systems applications would be interest.

To have directional radiations, reflectors are commonly used to design antennas, which are composed of radiating element and reflector. The common reflector is perfect electric conductor (PEC) and it can achieve a good unidirectional performance. However, there are drawbacks. Firstly, the overall

The associate editor coordinating the review of this manuscript and approving it for publication was Chan Hwang See.

profile of the directional antenna utilized PEC reflector is high. Since the reflection phase of the PEC is 180° for a normal incident wave, the distance between the radiating element and the metal reflector should be $\lambda/4$ to avoid destructive interference of the reflected wave and radiated wave. Secondly, the PEC reflectors are usually much larger than the radiating elements. Besides, its bandwidth is limited owing to the restriction of $\lambda/4$ distance. In recent years, as metamaterials are proposed, such as Electromagnetic Bandgap (EBG) and Artificial Magnetic Conductor (AMC) structures, the radiation characteristics of the antenna is improved and its profile is low [8]–[11]. The EBG is a periodic structure with high impedance [12] in a limited frequency range, which can suppress surface wave propagation and provide a better performance for the directional radiation. An EBG structure also operates as AMC in certain band. Also, the AMC is a periodic structure and operates with 0° reflection phase within a limited frequency range, which results in low-profile [12] antenna when it is applied as the antenna's reflector. However, an AMC cell is a high-Q resonator and its in-phase reflection band is narrow. Besides, it needs multiple periodic units, which makes the structure a large size. Another way to obtain directional radiating antennas is using Frequency Selective Surfaces (FSS) [13], [14]. In [13], a directional ultra-wide band antenna using dual-layer Frequency Selective Surface (FSS) reflector is designed, and it achieves an experimental bandwidth of 122% with gains about 7.5 dBi from 3 to 7 GHz and 9dBi ±0.5dB in 7-14 GHz. The composite structure is compact, with a total height of $\lambda/4$ (λ is the free-space wavelength at the lowest operating frequency of 3 GHz). In [14], a directional ultra-wide band antenna using multi-layer FSS reflector with a profile of 19 mm (0.19λ, λ is the free-space wavelength at the lowest operating frequency of 3 GHz) is presented, and it provides a wide bandwidth of 3-15 GHz with a peak gain of 9.3 dBi. The FSS provides reflection-phase coherence (at the antenna plane) in a quit wide band and the antennas obtain good performances, however, there are some drawbacks. Firstly, the FSS is a periodic structure, and muti-periods are necessary for its function, which may result in a large size. For example, the sizes of the FSS in [13] is $1.19\lambda \times 1.19\lambda$. Also, multi-layer structure may complicate an antenna.

In [15], the concept of a novel reflector, resonance-based reflector (RBR), is proposed. A prototype of the RBR of ring shape was also discussed in [15]. The RBR in [15] named ring-shaped RBR is composed of a metallic ring attached on a substrate, which achieves an in-phase reflection band ($-90° < \varphi < 90°$) from 1.97 GHz to 4.94 GHz (85.96%) and the reflection magnitude values ($|S_{11}|$) range from -0.3 dB to −18.7 dB within the in-phase reflection band. The Case 2 of the RBR antenna in [15] has a measured bandwidth of 87.11% (1.97-5.01 GHz). However, its FBR bandwidth is only 37.29% (2.16-3.15 GHz), even with a standard of FBR > 5 dB (the FBR values range from 5-16 dB in the band). Although the unidirectional antenna in [15] covers wide impedance bandwidth, the FBR values are low at high frequencies. In order to enhance the FBR values, a ring-shaped director (RD) was placed above a resonance-based reflector antenna to guide the high frequencies in [16]. The antenna in [16] covers a measured impedance bandwidth from 2.17-3.76 GHz (53.63%) and the FBR values range from 7-16 dB within the impedance bandwidth. The FBR bandwidth is wider and the FBR values are stable at high frequencies. However, the RD increases the profile. Moreover, with a standard of FBR > 10 dB, the bandwidth of the antenna in [16] is only 17.26%. In [17], an RBR antenna is proposed for wideband electromagnetic imaging. The RBR in [17] has meandered structure, which can increase the electrical size of the loop reflector without physically altering the dimensions of the substrate. The meandered RBR in [17] is applied to a perpendicular wideband dipole antenna, and it achieves a measured wideband unidirectional radiation from 0.83 GHz to 1.90 GHz (78.39%). Though the bandwidth is very large, its gains are small (with a peak gain of 3.8 dBi) and its FBR values are small (maximal FBR value is only 9 dB).

To overcome the drawbacks of narrow FBR bandwidths and low FBR values of the previous RBR antennas, a wide band RBR is proposed in this research. The proposed RBR consists of a metallic ring with three stubs printed on a substrate. Compared to the ring-shaped RBR in [15], the three stubs in this research affect the field distributions, and partial incident power is reflected by the stubs, which enhance the reflection. Therefore, the proposed RBR covers a wide in-phase reflection band ($-90° < \varphi < 90°$) from 3.23 GHz to 6.24 GHz (63.57%) and its reflection magnitude values range from −0.02 dB to −11.5 dB within the in-phase reflection band. Thus, the proposed RBR is superior to the ring-shaped RBR. The proposed RBR is mounted on a ring loaded teardrop-shaped bow-tie antenna (RBR-TBAR), and the proposed RBR antenna is formed. The measured FBR of the proposed RBR antenna is larger than 10 dB within the whole impedance bandwidth (3.48-6.12 GHz (55.00%)) and the maximum FBR is up to 20.4 dB. The measured peak gain is larger than 7 dBi within the whole impedance band. Compared to the previous RBR antennas, the proposed RBR antenna shows higher FBR value and wider FBR bandwidth [15]–[17], higher gain [17], and a lower profile without the need of a director [16]. The proposed RBR antenna provides a good directional radiation pattern and its profile is $0.15\lambda_L$ at the lowest operating frequency of the antenna. This paper is arranged as follows. The designing procedure is discussed in Section II. The design of the proposed RBR structure is provided in Section III. Section IV presents the simulated and measured results of the unidirectional antenna. Section V is a conclusion.

II. DESIGNING PROCEDURE AND CONCEPT OF THE RBR ANTENNAS

In the designing of uni-directional antennas; reflectors, such as PEC and AMC, are commonly used. The PEC has a reflection phase of 180°, which requires a distance of $\lambda/4$ between the radiator and the reflector. The AMC has a reflection phase

of 0°, which can be used to design very low-profile antennas. However, it operates at its resonance and turn out to be very narrow band, and it requires periodic structure. Moreover, the coupling between the radiator and the AMC would wreck the antenna performances. Therefore, a certain distance between the radiator and the AMC is usually required to weak the coupling the improve the antenna performances. The RBR reflector has a reflector phase between $-180° < \varphi < 180°$, therefore, the distance between the radiator and the RBR is in between 0 to $\lambda/4$. The RBR do not needed to be periodical and it is very wideband as it operates above its resonance. The designing procedures of the RBR antennas are as follow:

Step 1: The designing of an RBR structure. The RBR structure is usually a half-wavelength resonator. Then, its reflection phase is disturbed and ranges between $-180° < \varphi < 180°$ in a very wide frequency band above the resonance [15].

Step 2: Tailoring the RBR structure to achieve a large reflection magnitude in a wide frequency band. A large reflection magnitude is important to obtain good FBR.

Step 3: Defining a reference plane. The reference plane has a distance d from the RBR surface. The reflection phase is $-90° < \varphi < 90°$ at the reference plane.

Step 4: The designing of an UWB omni-directional antenna. The UWB antenna should have wide impedance bandwidth and compact size.

Step 5: The combining of the RBR structure and the UWB antenna. The UWB antenna is placed on the reference plane of the RBR structure. The parameters should be further optimized.

Through the above five steps, an UWB uni-directional RBR antenna can be successfully designed.

III. DESIGN OF THE PROPOSED RBR

Fig. 1 (a) is the schematic view of the reference ring-shaped RBR and Fig. 1 (b) is the schematic view of the proposed RBR. The proposed RBR is composed of a metallic ring with three stubs and they are printed on a F4B substrate with a thickness of 1mm and a relative permittivity $\varepsilon_r = 2.65$. The longest metallic stub is along the radial direction of the ring, while the other two equal metallic stubs are parallel to the longest stub with the distance of $R/2$. All the parameters of

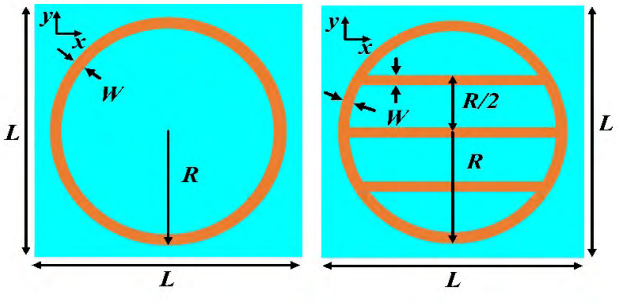

FIGURE 1. Schematic view of RBRs: (a) the reference RBR (b) the proposed RBR.

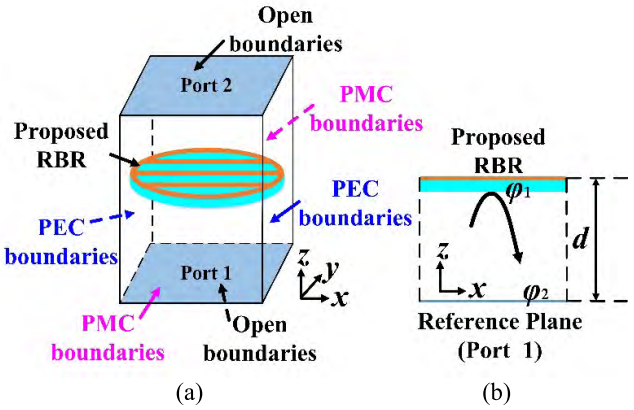

FIGURE 2. Schematic view of the simulation model for the proposed RBR: (a) model (b) reference plane.

the proposed RBR and the reference RBR are optimized as follows: $L = 54$mm, $R = 26$mm, $R/2 = 13$mm, $W = 1$ mm.

Fig. 2 (a) is the schematic view of the simulation model for the proposed RBR. As the RBR is a resonant structure, the characteristics of RBRs are dominated by its own resonance and the structure itself, thus, the periodicity has small impact on the characteristics [16], which means the coupling between RBRs is negligible. Thus, periodical boundaries can be set for the simulation model of the proposed RBR. It is set up with PEC boundary along the x-axis (to imitate the x-axis polarized wave), PMC boundary along the y-axis and open boundary along z-axis with the help of the electromagnetic full-wave simulation software, CST Microwave Studio. In addition, an air box is made and two wave ports are set up on the top and bottom (along z axis) of the air box to imitate infinitely long waveguides for reflection and transmission. The port 1 with distance d to the RBR surface is denoted as a reference plane and it produces an incident wave. Then, the reflection phase at the proposed RBR surface is denoted as φ_1 and the reflection phase at the reference plane is denoted as φ_2.

Assuming an uniform plane wave propagates from the reference plane to the RBR surface and reflects back to the reference plane. Then, the space phase shift is:

$$\Delta\varphi = -2\beta d. \tag{1}$$

where β is phase constant. The phase of the reflected wave at the reference plane is described by the following equations:

$$\varphi_2 = \varphi_1 + \Delta\varphi = \varphi_1 - 2\beta d. \tag{2}$$

In order to obtain in-phase coherence of incident and reflected wave at the reference plane, ideally $\varphi_2 = 0$ (or $2n\pi$, $n = 1, 2, 3\cdots$), the distance d is:

$$d = \frac{\varphi_1}{2\beta} = \frac{\varphi_1\lambda}{4\pi}. \tag{3}$$

It can also be written as:

$$d = \frac{\varphi_1}{2\beta} = \frac{\varphi_1 c}{4\pi f} \tag{4}$$

From the equations (3) and (4), $\varphi_1 = 0$ outputs $d = 0$. It is the case of AMC reflector. However, the there is still some distance between the AMC and the antenna owing to their coupling effect. And, the AMC usually has a narrow in-phase band. For, $\varphi_1 = \pi$, it is the case of PEC reflector and $d = \lambda/4$. For this case (RBR), $-180° < \varphi_1 < 180°$, the d should smaller than $\lambda/4$. The d can also be optimized by full-wave simulation to obtain the in-phase $-90° < \varphi_2 < 90°$ at the reference plane.

The reflection magnitudes and reflection phases of the proposed RBR and the reference RBR are shown in Fig. 3 for comparison. Fig. 3 (a) and (b) demonstrate the reflection magnitudes and phases at the RBR surfaces, respectively. From Fig. 3 (a) and (b), the reference RBR resonates at 1.93 GHz (the reflection magnitude is 0 dB) and the proposed RBR resonates at 3.35 GHz. It is also found from Fig. 3 (a), the proposed RBR obtains larger reflection magnitudes than the reference RBR in a wider band, which would be superiority as a reflector as discussed below. From Fig. 3 (b), the reflection phases at the surfaces of the RBRs are $0° < \varphi_1 < 180°$, which means their phases are in between the PMC (0°) and PEC (180°). Therefore, according equations (3) and (4), in a certain distance d from RBR surfaces, the reflection phases can be considered as in-phase ($-90° < \varphi_2 < +90°$). In this research, the optimal $d = 10$ mm. It can be found from Fig. 3 (c), the reference RBR covers the in-phase reflection band from 1.82 GHz to 3.62 GHz (66.18%), and the proposed RBR covers the in-phase reflection band from 3.23 GHz to 6.24 GHz (63.57%). Therefore, from Fig. 3 (a) and (c), the proposed RBR achieves a better reflection magnitude bandwidth within the in-phase reflection band. In Fig. 3 (a), the reflection magnitude for the proposed RBR exceeds −5 dB (31.62% energy of incident wave is reflected) from 3.23 GHz to 6 GHz (60.02%) within its in-phase reflection band, while the reflection magnitude for the reference RBR exceeds −5 dB from 1.82 GHz to 2.83 GHz (43.44%) within its in-phase reflection band. That means the proposed RBR possesses a greater reflection magnitude values within its in-phase reflection band and it would enhance the FBR bandwidth.

To reveal the operating mechanisms of the bandwidth enhancement of the proposed RBR, the surface current distributions at the resonant frequencies of the reference RBR and the proposed RBR are shown in Fig. 4 for comparison. It is seen from Fig. 4 (a), the surface currents for the reference RBR originate from one side and flow to the other side along the two semi-rings, respectively. As mentioned in [15], the reference RBR operates as two $\lambda/2$ resonators, then, the wavelength of the resonance f_r for the reference RBR ($\lambda_r = c/f_r = 155.44$mm) is almost equal to the equivalent perimeter of the ring ($2\pi \times (R\text{-}W/2) = 160.22$ mm ($1.03\lambda_r$)). From Fig. 4 (b), due to the introduction of the three stubs, parts of the currents and power of the two semi-rings are allocated to the three stubs. Part of the electromagnetic energy of the two semi-rings is coupled to the three stubs compared to the reference RBR, therefore, partial of the incident power is reflected by the stubs, which enhance the reflection. Besides, the semi-rings and the three stubs are in different sizes, which indicates reflection enhancement

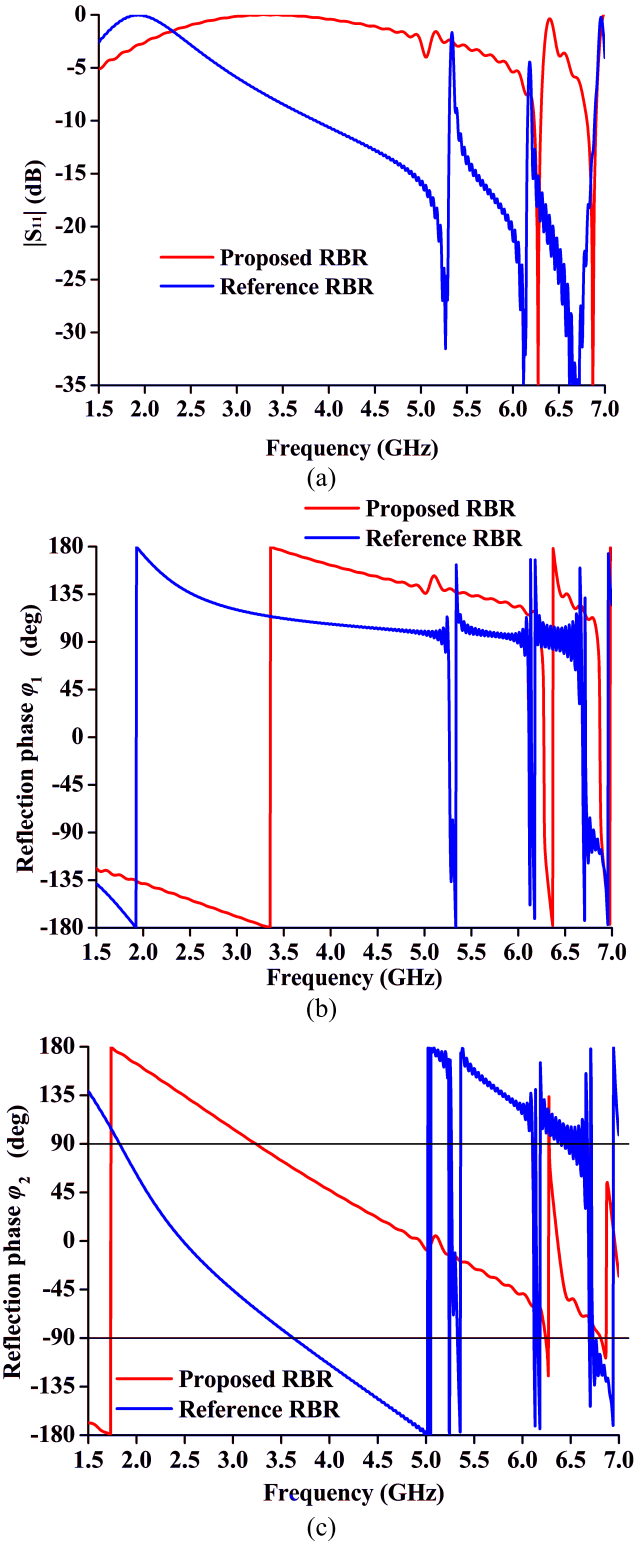

FIGURE 3. The reflection magnitude ($|S_{11}|$) and reflection phases of the proposed RBR and reference RBR: (a) reflection magnitudes ($|S_{11}|$) (b) reflection phases at the RBR surface φ_1 (c) reflection phases at the reference planes φ_2.

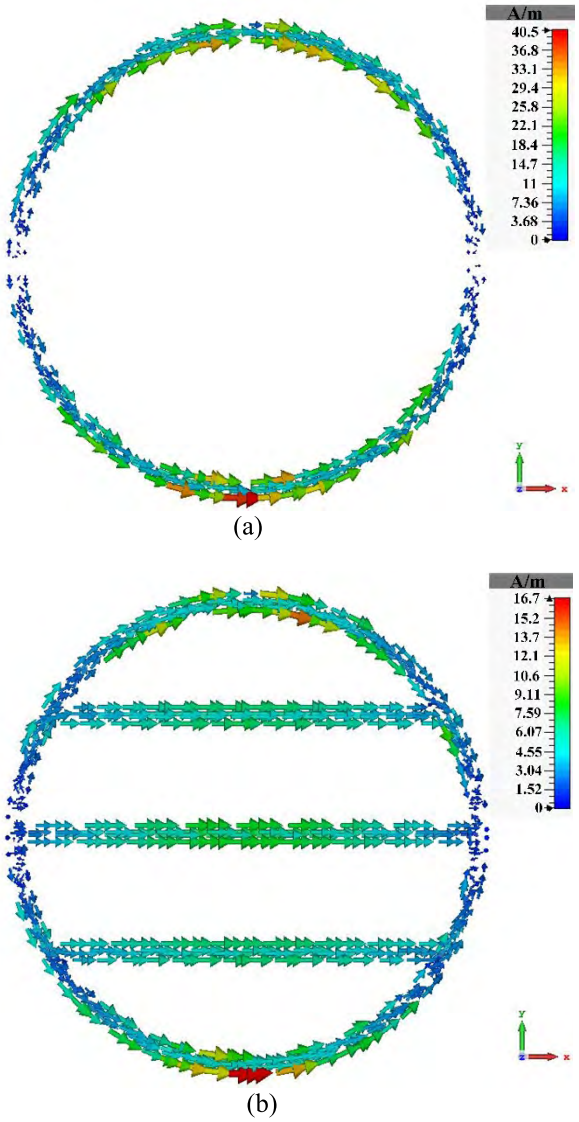

FIGURE 4. The surface currents distribution of the reference RBR and the proposed RBR at their respective resonance frequencies: (a) reference RBR (b) proposed RBR.

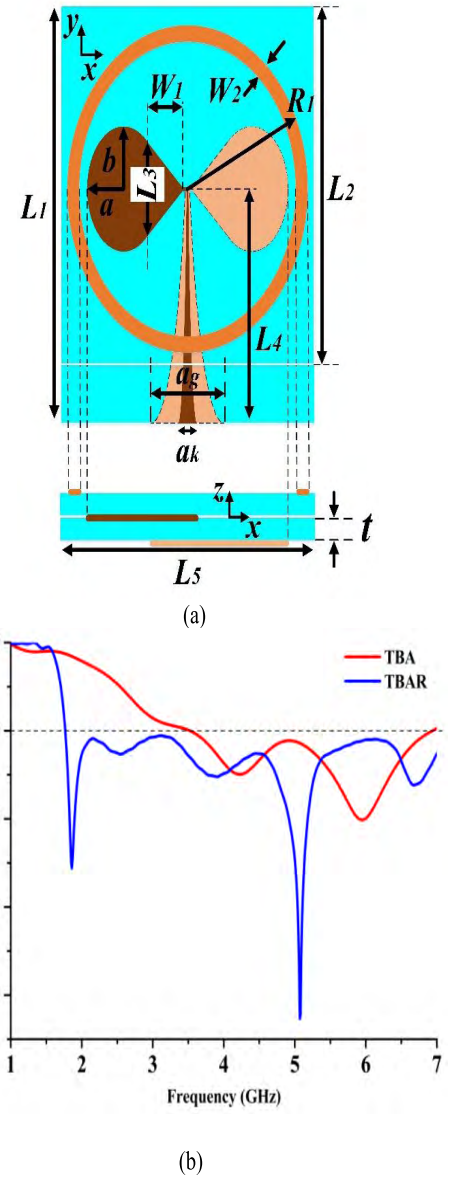

FIGURE 5. The reference bow-tie antenna: (a) structure (b) results.

in a wide band. Thus, the proposed RBR achieves greater reflection magnitude values within its in-phase reflection band. As mentioned above, the reflection magnitude for the proposed RBR exceeds −5 dB from 3.23 GHz to 6 GHz (60.02%), but the reflection magnitude for the reference RBR exceeds −5dB from 1.82 GHz to 2.83 GHz (43.44%) within their respective in-phase reflection bands. The former enhances bandwidth of 16.58% with the introduction of three stubs than the latter. It is also noticed that, as the current path is shortened by three stubs, the proposed RBR operates at higher frequencies. The wavelength of the resonance f_p for the proposed RBR ($\lambda_p = c/f_p = 89.55$mm) is not equal to the equivalent perimeter of the ring ($2\pi \times (R\text{-}W/2) = 160.22$ mm ($1.79\lambda_p$)). However, from Fig. 4 (b), the proposed RBR is still the composites of $\lambda/2$ resonators.

IV. DESIGN AND RESULTS OF THE PROPOSED RBR ANTENNA

A. THE PROPOSED RBR ANTENNA DESIGN

A bow-tie antenna is a planar antenna and it possesses many merits, such as small size, light weight, low cost, wide bandwidth, and an omnidirectional radiation pattern [18]–[20]. It is a good candidate for UWB wireless systems. On the contrary, a nonplanar bow-tie antenna named folded bow-tie antenna (FBA) is proposed for ground penetrating radar applications in [21]. In this paper, a planar bow-tie antenna is used as radiating element. The bow-tie antenna consists two symmetric teardrop-shaped patches. The smooth structure of the teardrop-shaped patches helps to smooth surface current and guarantee good impedance matching. The teardrop-shaped patches are printed on the two sides of a substrate

TABLE 1. The optimized dimensions of the TBAR.

Parameters	Dimensions (mm)	Parameters	Dimensions (mm)
a	8	L_4	44.6
a_g	12	L_5	54
a_k	1.5	R_1	26
b	10	t	1
L_1	71.6	W_1	7
L_2	54	W_2	1
L_3	15		

(as shown in Fig. 5 (a)), therefore, the patches can be fed by a microstrip line, whose impedance is transformed to 50Ω by a gradual balun, and the antenna can be fed by a coaxial SMA connector. As discussed in [22]–[23], a loading ring can reduce antenna size, improve impedance matching and radiating performance. Thus, a metallic ring is used in this research. As the bow-tie antenna is fed by a co-planar microstrip line, the ring has to be printed on another substrate as demonstrated in Fig. 5 (a). Both the substrates are F4B with a thickness of $t = 1$ mm and a relative dielectric constant of $\varepsilon_r = 2.65$. The $|S_{11}|$ curves for the teardrop-shaped bow-tie antenna (TBA) (without a loaded ring) and the TBA with a ring (denoted as TBAR) are shown in Fig 5 (b). As shown in the figure, the TBAR operates to a lower frequency (1.77 GHz) compared to the TBA (3.52 GHz). The optimized dimensions of the TBAR are shown in Table 1.

The proposed RBR is loaded to the TBAR with the optimized distance of $d = 10$ mm as Fig. 6 shown to realize unidirectional radiation. The antenna thickness is 13 mm. Four cylindrical plastic posts with the relative permittivity of $\varepsilon_r = 4$ are embedded between the TBAR and the proposed RBR to support the structures. The height (h) of the plastic posts are 19.22mm as depicted in Fig. 6. Note that, the balun fed to the bow-tie antenna in [15] is perpendicular to a reflector, which would be a restriction for some applications. In this design, the two symmetric teardrop-shaped patches are printed on the two sides of the substrate, so that the balun is parallel to the reflector, which can achieve a lower profile and size reduction. Note that, as the TBAR and the proposed RBR are assembled together, there is no returning work required for the structures.

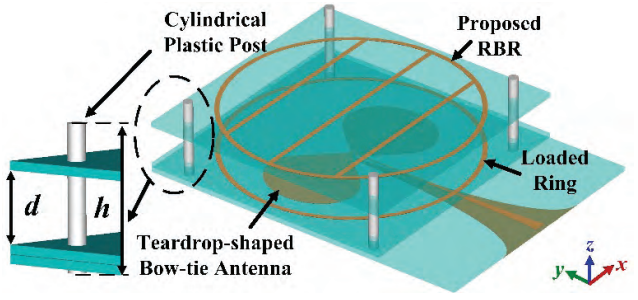

FIGURE 6. The schematic view of the proposed RBR loaded teardrop-shaped bow-tie antenna.

B. RESULTS AND DISCUSSION

The proposed RBR antenna is fabricated and measured as shown in Fig. 7. The dimensions of the antenna are $71.6\times54\times13$ mm^3 ($0.83\lambda_L\times0.62\lambda_L\times0.15\lambda_L$, λ_L is the lowest operating frequency of the antenna). Its $|S_{11}|$ was measured by the vector network analyzer (AV3656B) produced by China Electronics Technology Group Corporation (CETC)'s 41st Research Institute. Its radiation patterns, FBR and gain were measured by the NSI2000 system in an anechoic chamber. Fig. 8 shows the $|S_{11}|$ curves of the simulation and measurement. The proposed RBR antenna covers the simulated impedance bandwidth from 3.41 GHz to 6.22 GHz (58.36%), while the measured impedance bandwidth is of 3.48-6.12 GHz (55.00%). There is a good agreement between the measured

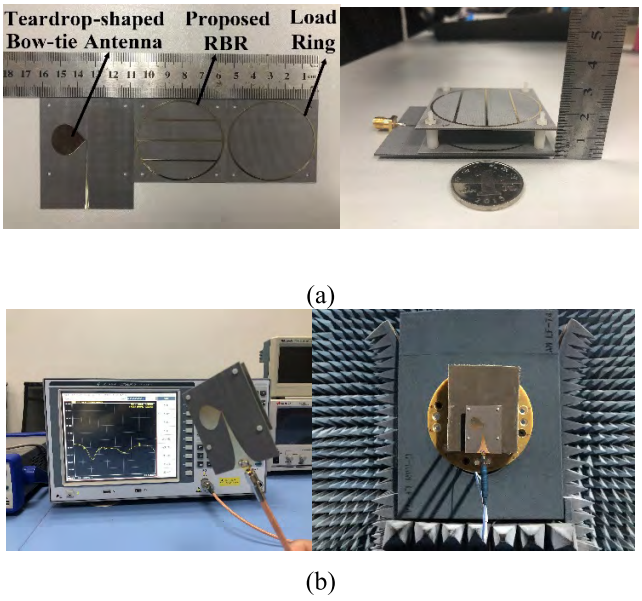

FIGURE 7. Prototype and measurement of the proposed RBR antenna: (a) manufactured prototype (b) measurement.

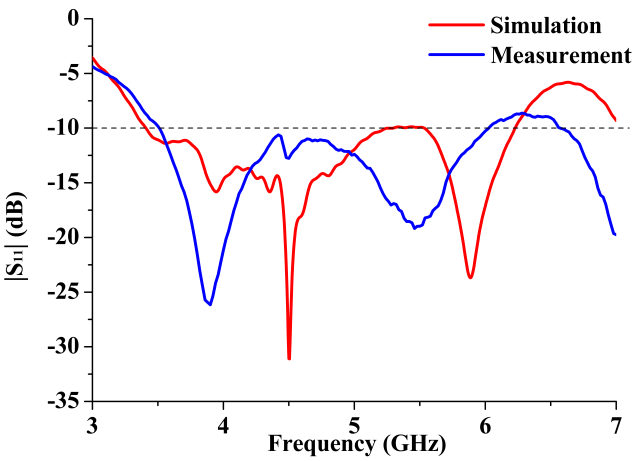

FIGURE 8. The $|S_{11}|$ curves of simulation and measurement.

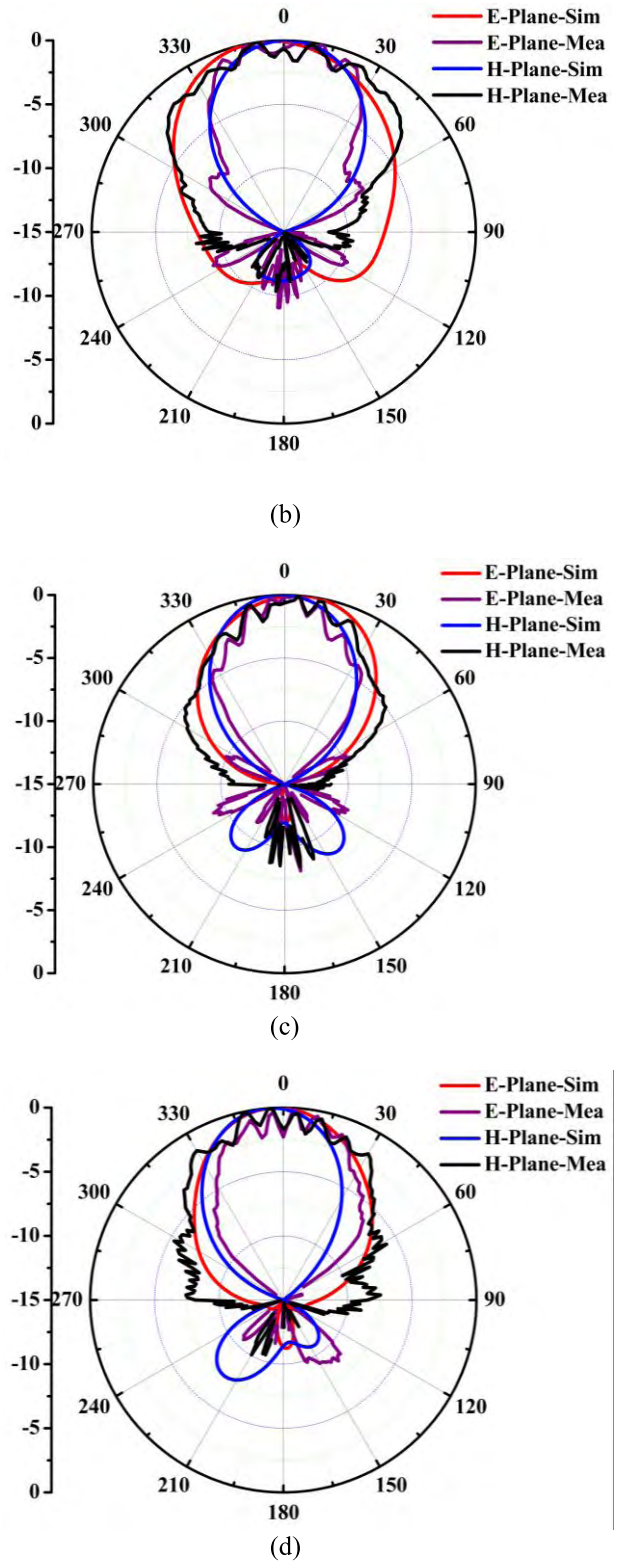

FIGURE 9. The radiation patterns of the proposed RBR antenna: (a) 4 GHz, (b) 5 GHz, (c) 5.5 GHz, (d) 6 GHz.

and simulated results except small deviations which is due to the limitations in fabrication and measurement setup.

Fig. 9 (a), (b), (c) and (d) shows the radiation patterns (E-Plane and H-Plane) of the proposed RBR antenna at 4, 5, 5.5, and 6 GHz, respectively. Owing to the limitation of the measuring environment, only a haft of the radiation pattern can be measured in a time, therefore, a front pattern and a back pattern are measured separately and made together to form a whole radiation pattern. Though discrepancies between the simulated and measured results are observed, there is still a reasonable agreement between the simulated and measured radiation patterns. And, both the simulated and measured patterns verify good unidirectional patterns at the four frequencies. It is found that all the direction of maximum radiation is slightly off the normal, which is due to the antipodal layout of the antenna itself [24].

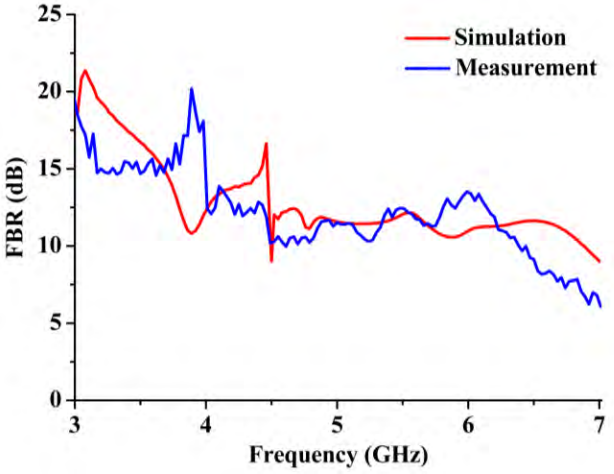

FIGURE 10. The FBR curves of simulation and measurement.

Fig. 10 shows the simulated and measured FBR curves. The FBR is defined as the ratio of the front radiation (0°) to the back radiation (180°). The measured FBRs are larger than 10 dB in the impedance matching band. Fig. 11 shows the simulated and measured peak gains. As shown in the figure, the simulated gains range from 6.8 dBi to 10.44 dBi in the operating band, and the measured gains range from 7.3 dBi to 9.03 dBi. Fig. 12 only shows the simulated directivity and efficiency of the proposed RBR antenna. The directivities are more than 6.8 dBi and the efficiencies are above 87.65% in the operating band.

The performances comparisons between the proposed RBR antenna and other designs in [8], [10], [13], [15]–[17], and [25] are given in Table 2. The antennas in [8] and [13] occupy large areas, and the antenna in [10] has a high profile. Besides, the FBR characteristics are not discussed in [8], [10], and [13]. The FBR bandwidths of the antennas in [15]–[17] and [25] are narrower than this design, even they are based on a lower FBR standard. For example, the antennas in [15] obtains an FBR bandwidth of 37.29%, even in a low FBR standard of 5 dB (FBR $>$ 5 dB). In [16], though additional director is used to enhance the FBR bandwidth (which complicates the structure and results in higher profile), its FBR

TABLE 2. The performance comparison between the proposed RBR antenna and other designs in [8], [10], [13], [15]–[17], and [25] (λ_L is calculated at the lowest operating frequency of antennas).

	Area (λ_L)	Profile (height) (λ_L)	Impedance Bandwidth (%)	FBR bandwidth (%)	Peak FBR (dB)	Peak Gain (dBi)	3dB Gain bandwidth (%)	Reflector types
[8]	2.48×0.71 (1×4 array)	0.17	24.4 (2.66-3.40GHz)	——	——	13.3	24.4	EBG
[10]	0.87×0.87	0.22	45.47 (3.84-6.10 GHz)	——	——	9.3	——	AMC
[13]	1.19×1.19	0.135	122 (3-12.38 GHz)	——	——	9.8	122	FSS
[15] (Case 2)	0.34× 0.34	0.11 (0.32 by considering the balun)	87.11 (1.97-5.01 GHz)	37.29 (FBR: 5-16 dB)	16	7.4	87.11	RBR
[16]	0.38× 0.38	0.16 (0.39 by considering the balun)	53.63 (2.17-3.76 GHz)	17.26 (FBR > 10 dB)	18	7.5	53.63	RBR
[17]	0.23× 0.23	0.28	78.39 (0.83-1.90 GHz)	(Max FBR value: 9 dB)	9	3.8	56.33	RBR
[25]	0.36× 0.36	0.16 ((0.41 by considering the balun))	126.53 (1.8-8 GHz)	FFB: 20 BFB: 46.9 (FBR > 5 dB)	FFB: 11.3 BFB: 20	FFB: 7.3 dBic BFB: 8.5 dBic	126.53	RBR
Proposed design	0.83× 0.62	0.15	55.00 (3.48-6.12 GHz)	55 (FBR > 10 dB)	20.4	9.03	55.00	RBR

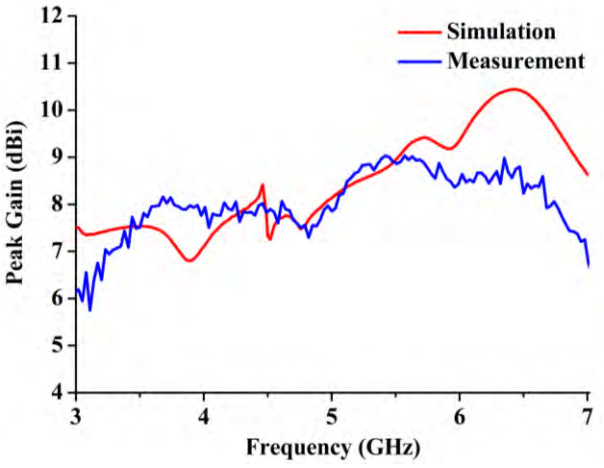

FIGURE 11. The peak gain curves of simulation and measurement.

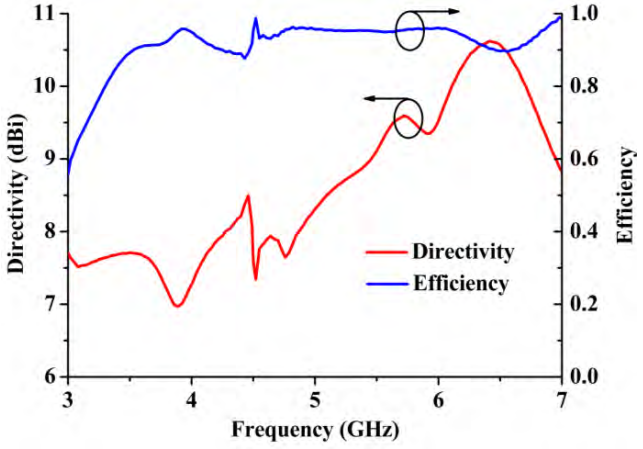

FIGURE 12. The simulated directivity and efficiency curves of the proposed RBR antenna.

bandwidth is only 17.26% with FBR > 10 dB. In [17], though the antenna presents uni-directional radiation in a very wide band, its FBR bandwidth is not mentioned, and its max FBR value is only 9 dB. In [25], the antenna utilizes two RBR and achieves two opposite uni-directional circular polarized radiation bands. One is the front-fire band (FFB) and the other is the back-fire band (BFB). The FBR bandwidths of the FFB and the BFB are of 20.0% and 46.9%, respectively, with a low FBR standard of 5 dB (FBR > 5 dB). In this design, the FBR bandwidth is up to 55% with a high FBR standard of 10 dB (FBR > 10 dB). Besides, the antennas in [15], [16], and [25] are fed by gradual baluns that is perpendicular to the

antennas, which would be negative effect for the profiles of the antennas. In this design, the antenna is fed by co-planar balun, which would be beneficial for some applications. From Table 2, this design has better peak FBR and peak gain values.

V. CONCLUSION

A wideband RBR is proposed in this paper and it has an in-phase band of 3.23-6.24 GHz (63.57%). The proposed RBR antenna achieves a measured wide impedance bandwidth from 3.48 GHz to 6.12 GHz (55.00%). The measured FBR is larger than 10 dB within the whole impedance matching band and the maximum FBR is up to 20.4 dB. The measured peak gain is more than 7.3 dBi within the whole band. It also achieves good unidirectional patterns and there is a good agreement between the measured and simulated results. The profile of the overall proposed RBR antenna is $0.15\lambda_L$ at the lowest operating frequency of the antenna and the simulated efficiencies are above 87.65% in the operating band. The proposed RBR antenna possesses the merits of compactness, good unidirectional performance, low-profile and enhanced FBR bandwidth. Therefore, the proposed RBR antenna is a good candidate for 5G systems applications.

REFERENCES

[1] W. Amer, G. Y. Tian, and C. Tsimenidis, "A novel, low-profile, directional UWB antenna for WBAN," in *Proc. Loughborough Antennas Propag. Conf. (LAPC)*, Nov. 2014, pp. 708–710.

[2] M. Klemm, I. Z. Kovcs, G. F. Pedersen, and G. Tröster, "Novel small-size directional antenna for UWB WBAN/WPAN applications," *IEEE Trans. Antennas Propag.*, vol. 53, no. 12, pp. 3884–3885, Dec. 2005.

[3] X. M. Qing and Z. N. Chen, "A miniaturized directional UWB antenna," in *Proc. IEEE Int. Symp. Antennas Propag. (APSURSI)*, Jun. 2011, pp. 1470–1473.

[4] R. Cavallari, F. Martelli, R. Rosini, C. Buratti, and R. Verdone, "A survey on wireless body area networks: Technologies and design challenges," *IEEE Commun. Surveys Tuts.*, vol. 16, no. 3, pp. 1635–1657, Aug. 2014.

[5] A. T. Mobashsher, "Wideband microwave imaging system for brain injury diagnosis," Ph.D. dissertation, Univ. Queensland, Brisbane, QLD, Australia, 2016.

[6] N. R. Zulkefly *et al.*, "Channel characterization for indoor environment at 17 GHz for 5G communications," in *Proc. IEEE 12th Malaysia Int. Conf. Commun. (MICC)*, 2015.

[7] K. L. Wong, H. J. Chang, and W. Y. Li, "Integrated triple-wideband triple-inverted-F antenna covering 617–960/1710–2690/3300–4200 MHz for 4G/5G communications in the smartphone," *Microw. Opt. Technol. Lett.*, vol. 60, pp. 2091–2343, Sep. 2018.

[8] S. Jam and M. Simruni, "Performance enhancement of a compact wideband patch antenna array using EBG structures," *AEU-Int. J. Electron. Commun.*, vol. 89, pp. 45–55, May 2018.

[9] C. Huang, C. Ji, X. Wu, J. Song, and X. Luo, "Combining FSS and EBG surfaces for high-efficiency transmission and low-scattering properties," *IEEE Trans. Antennas Propag.*, vol. 66, no. 3, pp. 1628–1632, Mar. 2018.

[10] Y. F. Cao and X. Y. Zhang, "A wideband beam-steerable slot antenna using artificial magnetic conductors with simple structure," *IEEE Trans. Antennas Propag.*, vol. 66, no. 4, pp. 1685–1693, Apr. 2018.

[11] Y. F. Cao, X. Y. Zhang, and T. Mo, "Low-profile conical-pattern slot antenna with wideband performance using artificial magnetic conductors," *IEEE Trans. Antennas Propag.*, vol. 66, no. 5, pp. 2210–2218, May 2018.

[12] D. Sievenpiper, L. Zhang, R. F. J. Broas, N. G. Alexopolous, and E. Yablonovitch, "High-impedance electromagnetic surfaces with a forbidden frequency band," *IEEE Trans. Microw. Theory Techn.*, vol. 47, no. 11, pp. 2059–2074, Nov. 1999.

[13] Y. Ranga, L. Matekovits, K. P. Esselle, and A. R. Weily, "Multioctave frequency selective surface reflector for ultrawideband antennas," *IEEE Antennas Wireless Propag. Lett.*, vol. 10, pp. 219–222, 2011.

[14] Y. Ranga, L. Matekovits, A. R. Welly, and K. P. Esselle, "A constant gain ultra-wideband antenna with a multi-layer frequency selective surface," *Prog. Electromagn. Res. Lett.*, vol. 38, pp. 119–125, Mar. 2013.

[15] L. Peng, J. Xie, K. Sun, X. Jiang, and S. Li, "Resonance-based reflector and its application in unidirectional antenna with low-profile and broadband characteristics for wireless applications," *Sensors*, vol. 16, no. 12, p. 2092, 2016.

[16] L. Peng, J.-Y. Xie, X.-F. Li, and X. Jiang, "Front to back ratio bandwidth enhancement of resonance based reflector antenna by using a ring-shape director and its time-domain analysis," *IEEE Access*, vol. 5, pp. 15318–15325, 2017.

[17] S. A. Rezaeieh, M. A. Antoniades, and A. M. Abbosh, "Compact and unidirectional resonance-based reflector antenna for wideband electromagnetic imaging," *IEEE Trans. Antennas Propag.*, vol. 66, no. 11, pp. 5773–5782, Nov. 2018.

[18] M. Midrio, S. Boscolo, and F. Sacchetto, "Novel ultra-wideband bow-tie antenna with high front-to-back ratio and directivity," *Microw. Opt. Technol. Lett.*, vol. 52, no. 5, pp. 1016–1020, May 2010.

[19] S. Kubota, N. Sasaki, and Y. Kayaba, "High gain and high directivity UWB bow-tie antenna with high impedance metamaterial surface," in *Proc. Int. Conf. Solid State Devices Mater.*, 2009, pp. 100–101.

[20] R. Xu, J.-Y. Li, and J. Liu, "Frequency-selective polarisation antenna based on simple rotational symmetric printed bow-tie dipole structure," *IET Microw., Antennas Propag.*, vol. 12, no. 7, pp. 1107–1111, Mar. 2018.

[21] M. Serhir and D. Lesselier, "Wideband reflector-backed folded bowtie antenna for ground penetrating radar," *IEEE Trans. Antennas Propag.*, vol. 66, no. 3, pp. 1056–1063, Mar. 2018.

[22] L. Peng, J. Y. Xie, X. Jiang, and S. Li, "Investigation on ring/split-ring loaded bow-tie antenna for compactness and notched-band," *Frequenz*, vol. 70, nos. 3–4, pp. 89–99, 2016.

[23] L. Peng, K. Sun, J. Y. Xie, Y.-J. Qiu, and X. Jiang, "UWB bi-directional bow-tie antenna loaded by rings," *J. Korean Phys. Soc.*, vol. 69, no. 1, pp. 22–30, Jul. 2016.

[24] M. Midrio, S. Boscolo, F. Sacchetto, M. Pascolini, F. M. Pigozzo, and A. D. Capobianco, "A novel UWB bow-tie antenna design with high F/B ratio and directivity," in *Proc. 38th Eur. Microw. Conf.*, Oct. 2008, pp. 393–396.

[25] J.-Y. Xie, L. Peng, B.-J. Wen, and X. Jiang, "Archimedean spiral antenna with two opposite uni-directional circularly polarized radiation bands designed by resonance based reflectors," *Prog. Electromagn. Res. Lett.*, vol. 70, pp. 23–30, Aug. 2017.

BAO-JIAN WEN was born in Guangxi, China, in 1989. He received the B.E. degree in communication engineering from the Chengdu University of Information Technology, China, in 2015. He is currently pursuing the master's degree with the Guilin University of Electronic Technology. His research interests include antennas and metamaterials.

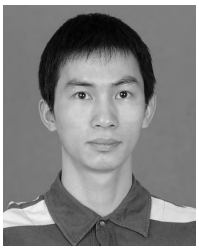

LIN PENG (M'16) was born in Guangxi, China, in 1981. He received the B.E. degree in science and technology of electronic information and the master's and Ph.D. degrees in radio physics from the University of Electronic Science and Technology of China, Chengdu, China, in 2005, 2008, and 2013, respectively.

From 2011 to 2013, he was a Joint Ph.D. Student with the University of Houston, sponsored by the China Scholarship Council. Since 2013, he has been with the Guilin University of Electronic Technology, where he has been an Associate Professor, since 2016. He has published over 30 papers as first or corresponding author. He has co-authored over 30 papers. His research interests include terahertz technologies, metamaterials/metasurfaces, antenna/filter theory and design, electromagnetic bandgap structure design and its application in antenna, composite right/left-handed transmission line and its applications, and conformal antenna array.

In recent years, he is sponsored by several funds, such as Fundamental Research Funds for the Central Universities, National Natural Science Foundation of China, Natural Science Foundation of Guangxi, Program for Innovative Research Team of Guilin University of Electronic Technology, and Guangxi Key Laboratory of Wireless Broadband Communication and Signal Processing. He serves as an Associate Editor for the IEEE Access. He also serves as a Reviewer for the IEEE Transactions on Microwave Theory and Techniques, the IEEE Transactions on Antennas and Propagation, IEEE Microwave and Wireless Components Letters, IEEE Antennas and Wireless Propagation Letters, *Electronics Letters*, *IET Microwave, Antennas & Propagation*, *IET Communications*, *Wireless Personal Communications*, *Progress in Electromagnetics Research*, *Electronics Letters*, and the *Journal of Electromagnetic Waves and Applications*.

XIAO-FENG LI was born in Shaanxi, China. He received the B.E. degree from Northwest Normal University, Lanzhou, China, in 1993, and the master's degree from Lanzhou University, in 2006. He is currently a Lecturer with the Guilin University of Electronic Technology. His research interests include antennas and electromagnetic measurements.

KUN-SHAN MO was born in Guangxi, China. He received the bachelor's and master's degrees from the University of Electronic Science and Technology of China, in 2010 and 2013, respectively. He is currently a Lecturer with the School of Electronic Information and Automation, Guilin University of Aerospace Technology. His research interests include antennas and microwave passive components.

XING JIANG received the master's degree in electromagnetic field and microwave technology from the Beijing Institute of Technology, in 1986. Since 2000, she has been a Professor with the Guilin University of Electronic Technology. She has published over 30 papers. Her research interests include smart communication system design, conformal antenna array, and bio-electromagnetics. She was also sponsored by the National Natural Science Foundation of China and the Natural Science Foundation of Guangxi. She is a Senior Member of the China Communications Society and a member of the Chinese Institute of Electronics.

SI-MIN LI received the B.S. degree in wireless communication engineering from the Nanjing University of Posts and Telecommunications, China, in 1984, and the M.S. and Ph.D. degrees in electronics engineering from the University of Electronic Science and Technology of China, Chengdu, China, in 1989 and 2007, respectively. From 1984 to 1986, he was an Engineer Assistant with the Optical Communication Department, Wuhan Post-Telecommunications Science and Research Institute. From 1989 to 2005, he was a Lecturer, an Assistant Professor, and a Professor with the School of Information and Communication, Guilin University of Electronic Technology. He is currently the President and a Professor with the Guangxi University of Science and Technology, Liuzhou, China. His current research interests include the design of electrically small antennas, antenna arrays for high-frequency communication systems, and wireless sensor networks.